

Using Adaptive Optics to Probe the Dynamics and Star Formation in Active Galactic Nuclei

Richard Davies, Linda Tacconi, Reinhard Genzel, Thomas Ott, and Sebastian Rabin
Max Planck Institut für extraterrestrische Physik, 85741 Garching, Germany

ABSTRACT

Using adaptive optics on the Keck Telescope and the VLT, we are able to probe the dynamics and star formation in Seyfert and QSO nuclei on spatial scales better than $0.1''$ in the H- and K-bands. Such spectroscopic data are essential for studying the link between AGN and star formation, understanding how gas is driven into the nucleus, and measuring the black hole mass. In this contribution we present some of our recent results, and consider what an astronomer needs from an adaptive optics system for extragalactic work, as well as what is realistic to expect. We discuss why deconvolution is not appropriate in this context; and examine the scientifically more useful alternative of convolving a model with an estimate of the PSF, describing what level of detail and reliability can actually be achieved in the various methods of measuring the PSF.

Keywords: Active Galactic Nuclei, Spectroscopy, Adaptive Optics, Point Spread Function, Convolution

1. INTRODUCTION: AN ALTERNATIVE VIEW ON MEASURING THE PSF

It is often said of adaptive optics data that one needs to make regular measurements of a point-spread function (PSF) reference, and use this to deconvolve the data. Unfortunately, for observations of active galactic nuclei (AGN) – particularly spectroscopic data – this is not practicable: observing a PSF reference is exactly what the astronomer does not want to spend precious observing time doing; and if one is observed, attempts to use it to deconvolve the data can often be suspect. There are a number of reasons for this:

- While intrinsically luminous, most AGN are far enough away that they appear rather faint. As a result, with the AO systems available on 8-m class telescopes, one cannot assume that the data will be diffraction limited. In order to provide an estimate of the resolution, any PSF reference must also be faint, resulting in either poor signal-to-noise or considerable lost observing time. Although in principal one could avoid this problem by observing a bright star and using blocking filters to reduce the counts on the wavefront sensor, there is in fact very limited capability for doing so in current systems.
- The surrounding stellar absorption and narrow line region emission features are much fainter than the AGN itself, and further diluted by its PSF halo. As a result, long integration times (at least several hours) are needed to obtain even barely sufficient signal-to-noise to make any useful measurements. Since it is impractical to stop frequently to make measurements of a PSF reference (which take typically 15–20 mins for even a few seconds integration each time), ‘snap-shot’ view that any PSF reference gives will probably be rather different from that associated with the AGN which is an average over the full period.
- At optical wavelengths, the core of an AGN may be slightly resolved (e.g. as is the case for NGC 1068). Additionally, there will always be underlying extended emission from the host galaxy. Both of these affect the AO performance in ways which are difficult to quantify and impossible to reproduce in a PSF reference. This is less of a problem for infrared wavefront sensors, but there are only a very few AGN which can be observed in this way without losing too much light from the science camera.

In this contribution we discuss various alternative ways of estimating the shape of the PSF that can be applicable to (spectroscopic) observations of AGN. All of these have disadvantages, but when two or more can be used together, they provide a reasonable degree of certainty about the result. We consider whether deconvolution is a viable option for post-processing, and what the alternative is. The scientific results that can be obtained when these issues are addressed is illustrated for two particular AGN: NGC 7469 and Mkn 231.

Further author information send correspondence to R.Davies:
E-mail: davies@mpe.mpg.de

2. ESTIMATING THE POINT SPREAD FUNCTION FOR ACTIVE GALACTIC NUCLEI

It hardly needs to be said that the ability to quantify the shape of the PSF for AO observations of AGN is crucial to a reliable interpretation of the data. However, the level of accuracy with which the PSF has to be known depends on what one is trying to achieve. In the most common cases this might simply be asking whether the core of the AGN is resolved – e.g. to determine the size-scale of the inner edge of the putative torus around the AGN itself; or to measure the radial luminosity profile – e.g. to determine whether it is more typical of a spheroid or disk. In these cases, the PSF does not have to be highly accurate; but it is important to have a good measurement of the width of the PSF's core (i.e. the actual spatial resolution) and the extent and brightness of its extended halo (i.e. how much a bright point source contaminates the surrounding emission). While these aims are often straightforward to achieve when the AO system is correcting on a star, the situation for an AGN is considerably more uncertain.

2.1. Observing a Separate Reference Star

We have already seen in Section 1 that estimating the PSF from a star observed at a different time from and with different characteristics to the target has numerous pitfalls, and should be treated with caution.

2.2. Using a Star in the Target Field

Using a star which serendipitously lies in the target field is initially an attractive option, and has been used successfully in at least one case.¹⁴ However, with current 1024×1024 detectors, the field of view obtained at AO pixel scales is rather limited: typically $30''$ if the K-band PSF is Nyquist sampled. With a few exceptions, such as the Circinus galaxy which lies close to the Galactic Plane, one is unlikely to find any suitable stars.

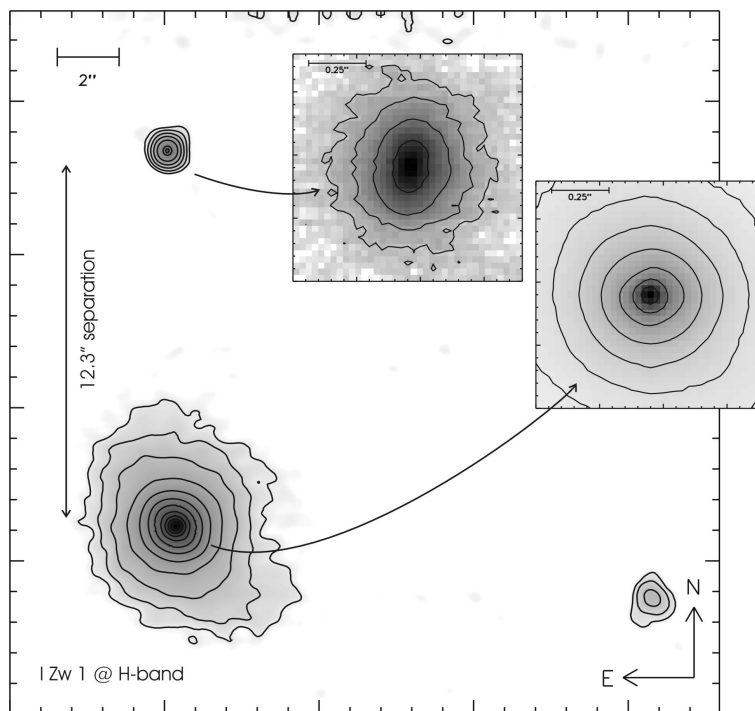


Figure 1. H-band image of I Zw 1 (adaptively smoothed; contours at factor 2 intervals), showing two off-nuclear continuum sources roughly due east and north. The insets show blow-ups of the nucleus (unresolved) and the northern source. It is unclear whether the size and shape of the latter is due to anisoplanatic effects – i.e. whether the northern source is an unresolved nearby star or whether it is a resolved stellar cluster lying in the disk of I Zw 1.

IZw 1 is an interesting example, since it has what has been taken to be a field star just $12.3''$ north of its nucleus. However, as shown in Fig. 1, H-band imaging with NACO has resolved this source, which has $H=15.4$ mag, to have a FWHM size of $0.20''$ (transversially) and $0.28''$ (radially). It clearly cannot be used as a PSF reference; and since there was only a single such off-nuclear point source in the field, the question has now become: can isoplanatic effects account for the size and shape of the source (which is oriented radially from the nucleus), or is it really resolved? The isoplanatic patch at the VLT can be rather small – and other observations suggest that during at least parts of this night it was – and sizes of less than $10''$ in the H-band are not rare. Its radial orientation from the wavefront sensor reference (its long axis points only $2''$ east of the nucleus) would suggest that the atmosphere is responsible for the shape. But if the source is intrinsically extended and lies at the distance of IZw 1, then it would have a projected size of over 240 pc and (assuming continuous star formation over a timescale of 100 Myr) a mass of $2 \times 10^8 M_{\odot}$ with a bolometric luminosity of $3 \times 10^{10} L_{\odot}$. This would be an important result, since it would make the cluster far larger than even the more massive star clusters typically seen in galaxies, and more comparable to what one might expect from a tidal dwarf galaxy, or possibly even the progenitor of the galaxy with which IZw 1 has been interacting. With the current data, it is not possible to be certain which of these is the correct interpretation.

2.3. Assuming the AGN is Unresolved

In only two cases has the core of an AGN been resolved in the K-band continuum: Circinus¹⁴ at a distance of 4 Mpc has a FWHM of $0.11''$ (1.9 pc), and NGC 1068^{17, 19, 23} at a distance of 14.4 Mpc has FWHM of $0.03''$ (2.1 pc). Given that the nuclear spectrum of such AGN is typically of that expect for hot dust grains (e.g. NGC 1068 is well represented by a black-body with a characteristic temperature of ~ 900 K^{4, 10, 19}), it is presumed that this core component is associated with the obscuring torus around the AGN. The majority of other AGN are significantly further away and, if 2 pc is the typical size of the core in the K-band, it seems reasonable to assume that it will be unresolved on scales similar to the diffraction limit of an 8-m telescope at these wavelengths. For example, NGC 7469 (Section 4) is at 66 Mpc and Mkn 231 (Section 5) is at 170 Mpc – for these two one would expect the K-band core of the AGN to have FWHM of only 6 mas and 2 mas respectively. This conclusion holds also for the H-band.

It is therefore reasonable to presume that the AGN core provides a good representation of the PSF. One has to be careful of nuclear continuum emission associated with star formation. However, in the cases we have examined this typically contributes to the peak surface brightness at less than the 10% level. We have found that fitting a combination of a Gaussian (to represent the unresolved core) and a Moffat profile (to represent jointly the halo of the core and the extended stellar continuum) provides a very good match to the observed continuum profile. The FWHM of the Gaussian component can then be taken as representative of the spatial resolution achieved.

The limitation of this method is that it does not provide any information about the the halo of the PSF, which can be very significant since the AO correction is only partial. As shown in Fig. 2, the halo dominated the radial profile of this NACO image of NGC 1068 out to radii of nearly $1''$.

2.4. Measuring the Slope of the Continuum

In the previous case we showed that the near infrared light from an AGN was produced by hot dust rather than stars and in most cases would be unresolved. Under this assumption, we can in principle use the slope of the continuum to measure the PSF: that part with a steep red slope will be due to the unresolved core, while the stars (which are typically dominated by late types) produce a bluer continuum.

One can adopt an iterative procedure to decompose the continuum into its stellar and thermal (hot dust) components in each spatial row of the spectrum. Initially, we assume that all the flux in the spatial row where the continuum is a maximum is due to hot dust and make an initial estimate of its temperature by calculating the spectral shape of the hot dust component and comparing it to that observed. The second step needs in addition a stellar template of a late type star. For NGC 7469 we used the K1.5 Ib HR 8465,²¹ although the exact type does not matter as the slopes of all cool stars are similar. These two components are scaled to match as well as possible the observed continuum spectral shape in each other row of the spectrum. The stellar cluster can then be traced through the scaling applied to the stellar template, which yields a smooth profile except for the

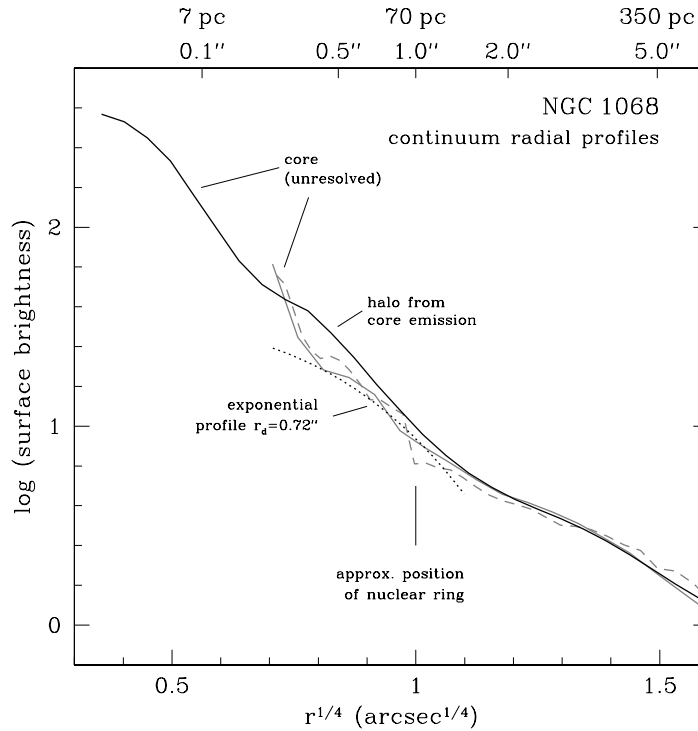


Figure 2. K-band radial profiles of NGC 1068. The black solid line is the azimuthally averaged profile from a VLT NACO image; the grey lines are the profiles found by fitting ellipses (dashed line) and the azimuthal average (solid line) from an HST NICMOS image. The black dotted line shows the best representation of the actual profile at radii 0.4–1.0", from the stellar absorption features. This matches the NICMOS profiles, but not the NACO profile which is still dominated by the wings of the core at these radii.

few rows near the centre. One can interpolate over these to estimate what the stellar contribution in this region should be. Subtracting this from the continuum of the central row used in the initial step leaves something that is closer to the original assumption that (the remaining spectrum in) this row is pure hot dust, and allows one to make a new estimate of the hot dust temperature. The procedure is repeated until the fit converges.

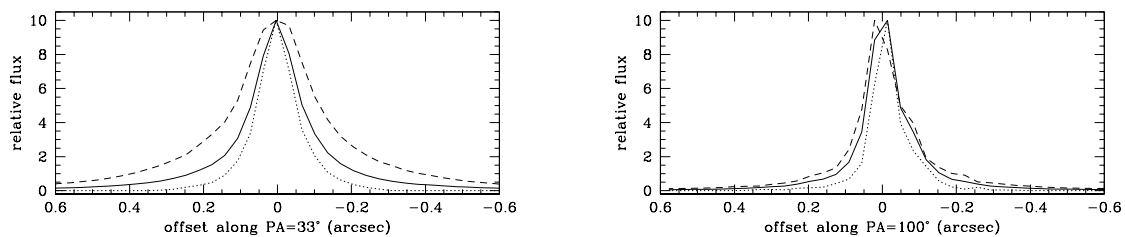


Figure 3. Profiles derived from fitting hot dust and a stellar template to the continuum spectral shape across the nucleus of NGC 7469 (at position angles 33° left, and 100° right). The solid line is the observed continuum profile, the dashed line the derived stellar cluster profile, and the dotted line the derived profile of the hot dust core (i.e. the PSF profile).

The results of the procedure for NGC 7469 are shown in Fig. 3: the hot dust core (dotted line) has a narrower profile than the observed continuum (solid line), and provides a measure of the spatial resolution achieved. At PA 33° (first night), its FWHM is 118 mas, compared with 146 mas for the full continuum; at PA 100° (second night), its FWHM was 80 mas (cf. 104 mas for the full continuum), similar to that measured on the separate

PSF reference.

Because this process uses the whole slope of the continuum, it provides a high signal-to-noise measurement of the spatial profiles of the hot dust core and stellar cluster. On the other hand, it is rather sensitive to errors in the slope of either the object spectrum or the standard star used to calibrate out atmospheric features. It also requires that the PSF is spatially well-sampled (better than Nyquist) so that the spatial gradients across the nucleus are not too steep. If this is not satisfied, then the interpolation (which one has to perform to straighten the spectra and apply wavelength calibration) can lead to errors in the spectral slope.

2.5. Using the Stellar Absorption Features

Another method which makes use of the unresolved nature of the AGN core is based on the stellar absorption features, and particularly the $1.62\ \mu\text{m}$ CO 6-3 or $2.29\ \mu\text{m}$ CO 2-0 bandheads. The CO absorption ‘flux’ is a direct tracer of late type stars and, in contrast to the equivalent width W_{CO} , is independent of dilution by hot dust. The rather stronger statement that the CO absorption flux traces the luminosity and mass profile of the stars can be made under the assumption that the CO equivalent width of the stellar type dominating the stellar continuum is constant across the entire region over which the absorption features are detected. In the H-band this is not so unlikely: the equivalent width of the CO 6-3 bandhead measured in the range $1.617\text{--}1.623\ \mu\text{m}$ lies in the range $3\text{--}5\ \text{\AA}$ for all K and early M type giant and supergiant stars.³

If the nuclear stellar profile is roughly uniform, then W_{CO} will depend only on the amount of dilution, and hence trace (in inverse) the profile of the hot dust causing the dilution, i.e. the PSF. However, in all the cases we have looked at so far,²⁻⁴ the nuclear stellar cluster is cusped, having an exponential profile and a disk scale length of less than $0.5''$. This means that while W_{CO} can be a guide to the resolution, and also give a good indication of the strength of the PSF’s halo (via the off-nuclear dilution), it cannot provide highly quantitative results. If the resolution is comparable to the width of the stellar cluster, the PSF estimate is relatively poor. On the other hand, the better the resolution, the better the estimate this method yields – since the core becomes ever narrower with respect to the extended stellar cluster.

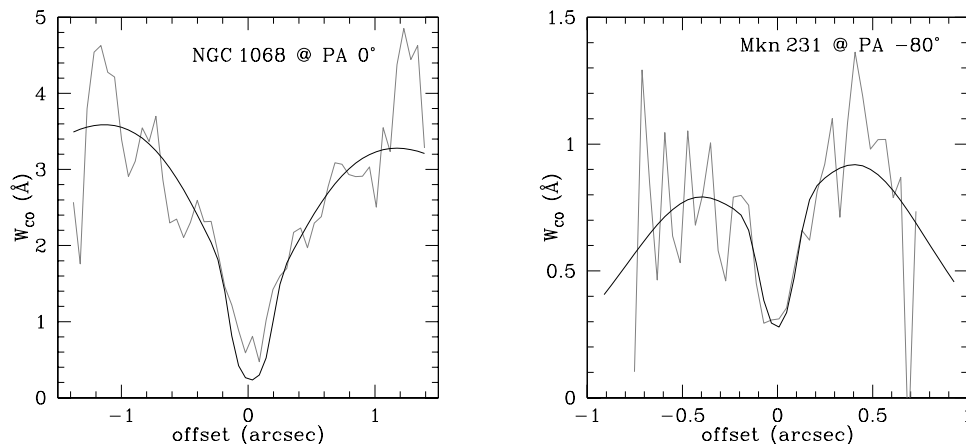


Figure 4. Spatial profiles of the CO 6-3 equivalent width in NGC 1068 (left) and Mkn 231 (right). The black line is the ratio derived from fitting functions to the continuum and CO absorption profiles; it is asymmetrical due to small (non-significant) offsets in the centering positions. In both cases the spatial resolution is seen to be of order $0.2''$; but since this is comparable to the widths of the stellar clusters, the method does not (in these cases) yield very quantitative estimates. In Mkn 231 the low W_{CO} does indicate that there is significant dilution (i.e. PSF halo light) even beyond $0.5''$ from the centre. The reduction in W_{CO} at the largest radii shown is an artifact of the different profiles used to trace the continuum and CO absorption, and is not a real effect.

Two examples are given in Fig.4. For NGC 1068 (left), the FWHM is of order $0.2''$, and there is little to no dilution beyond $\sim 0.5''$; For Mkn 231 (right), the FWHM is also of order $0.2''$, and there is strong dilution from the nucleus even beyond $0.5''$. This gives an indication that at these radii, the continuum is still tracing the PSF

rather than the stellar profile and provides one reason why the continuum does not yield a good match to the luminosity profile of the stellar cluster.

2.6. Using the Wavefront Sensor Gradients

From an astronomer's perspective, reconstructing the PSF (or an approximation to it) from the wavefront sensor gradients would be the most satisfactory method. Despite some effort in this direction (eg tests of a prototype on the ALFA system²²), there is as yet no such reconstructor installed in an AO system on an 8-m class telescope. However, some reconstructors are now under development (e.g. several contributions to this proceedings^{11, 12, 15}).

3. CONVOLVE OR DECONVOLVE ?

There are a variety of regimes for which deconvolution provides an ideal method to improve the spatial resolution beyond that attained directly. Two examples are images of star clusters – i.e. assemblies of point sources for which one wants to know flux and/or position; and images of planets or their moons – i.e. bright extended sources across which there is structure that cannot be described by a simple analytical function. In both cases it is usually possible to obtain a relatively large number of short exposure frames so that blind/myopic deconvolution also becomes a possibility, relieving the necessity of having a good PSF reference.

The situation for AGN, and indeed for much extragalactic work, is rather different. A poorly defined PSF, relatively few long exposure frames, limited signal to noise, and smooth extended emission punctuated by weak features all tend to make the results of deconvolution uncertain. For example, typically after a few iterations (~ 20) of the Lucy method, the noise is amplified into distinct features.

One of the primary analyses performed on images (or equivalently the spatial profiles of spectra) of galaxies is to quantify their morphology. In many cases this involves finding the best match among a number of model profiles which can be related directly to physical properties of the galaxy – for example to differentiate between a de Vaucouleurs $r^{1/4}$ profile usually given as $I(r) = I_e \exp\{-7.67[(r/r_e)^{1/4} - 1]\}$ which is characteristic of elliptical galaxies and bulges, or a simple exponential profile $I(r) = I_0 \exp\{-r/r_d\}$ typical of disks (note that for this profile the effective radius, inside of which half the total light is emitted, is 1.68 times the disk scale length r_d). The more general family of $r^{1/n}$ Sersic profiles $I(r) = I_0 \exp\{-b_n(r/r_e)^{1/n}\}$, in which the index of the exponent is left as a free parameter (so that $n = 4$ gives the de Vaucouleurs profile and $n = 1$ the simple exponential) can also be useful; the parameter b_n depends on n and is set by the requirement that the effective radius r_e marks the boundary that contains half the total light. It has been suggested that the index n of the Sersic profile is tightly correlated with the mass of the massive nuclear black hole.⁶

In general, as long as there is a physical model that one wishes to test, the best approach is to convolve that model with the best estimate of the PSF and then compare the result to the observations. This avoids the problems of deconvolving noisy data, or of trying to estimate the resulting PSF after deconvolution; and it has the added advantage of providing a more reliable estimate of the range of models that could reasonably fit the observations.

4. MULTIPLE RINGS IN NGC 7469

The Seyfert 1 galaxy NGC 7469, at a distance 66 Mpc, is a luminous infrared source with $L_{\text{bol}} \sim 3 \times 10^{11} L_{\odot}$. Much of the interest in the galaxy has been focussed on the circumnuclear ring structure on scales of 1.5–2.5'', which has been observed at many wavelengths. These data suggest that recent star formation in this ring contributes more than half the galaxy's bolometric luminosity. Additionally, up to 1/3 of the K-band continuum within 1'' of the nucleus may also originate in stellar processes.^{7, 13} NGC 7469 is therefore a key object for studying the relation between circumnuclear star formation and an AGN, and how gas is driven in to the nucleus to fuel these processes. Bringing together the unique combination of high resolution mm CO 2-1 data from the IRAM Plateau de Bure interferometer and near infrared adaptive optics H₂ 1-0S(1) data from the Keck II telescope, gives us a tool which can probe the distribution and kinematics of the molecular gas across nearly 2 orders of magnitude in spatial scale. Here we summarise our results, which are described fully elsewhere.²

Our 0.7'' 228 GHz CO 2-1 data of NGC 7469 show a number of distinct components: a broad disk; a ring of molecular clouds at a radius of 2.3'', located outside the well-known ring of star forming knots; a bar or loosely

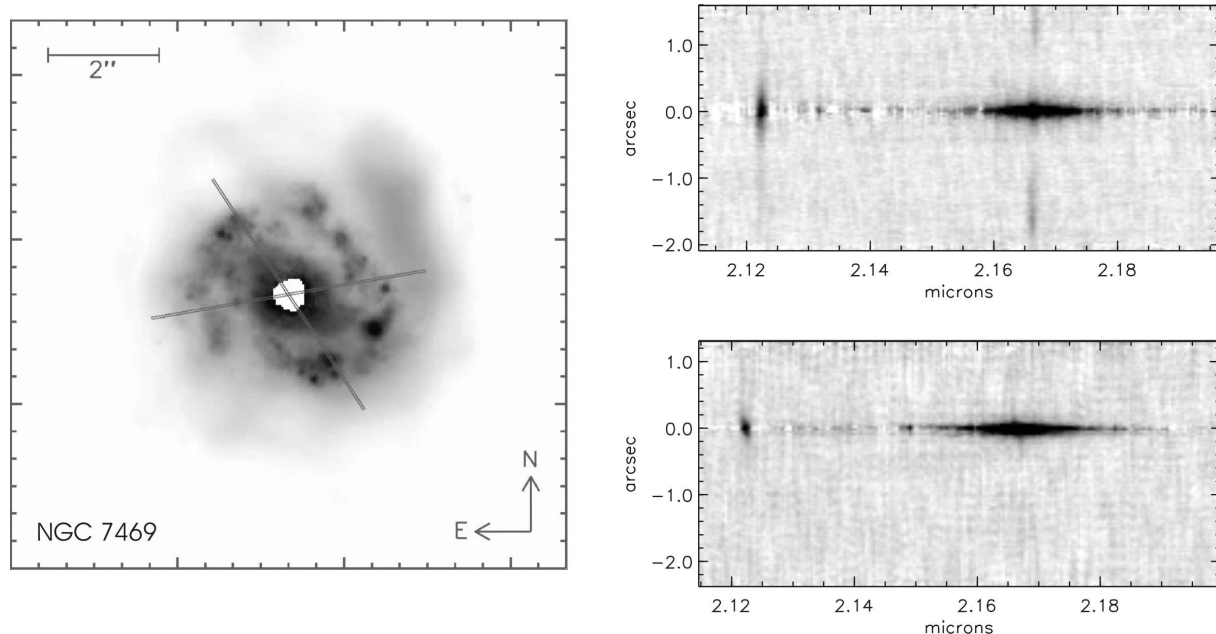


Figure 5. Left: overlay showing the stellar (J-band, kindly provided by A.Evans; dark knots) light on the gas (CO 2-1; smooth grey) distribution. The ring of star-forming knots lies mostly inside the ring of gas clouds. The central region where the nuclear light is strong has been masked out. Right: K-band position-wavelength spectra for the two slits, the positions of which are shown in the left-hand image. The broad Br γ line is clearly visible, as are extended narrow Br γ and hot H $_2$ 1-0S(1) line both of which exhibit velocity gradients.

wound spiral arms leading in from the ring; and an extended nucleus which, based also on the AO data, we interpret as a ring at radius 0.2''. An axisymmetric disk model is able to replicate the kinematics of this cold molecular gas, as well as the hot molecular gas traced by the 1-0S(1) line at much higher spatial resolution. The latter is shown in Fig. 6 which emphasizes the extended nature of the nucleus: if it were compact, the rotation curve would be much steeper than is observed. In contrast to the mass, the 1-0S(1) flux is compact, indicating that it does not trace the gas distribution. It is likely that the core 1-0S(1) arises in gas excited by UV and X-ray irradiation from the AGN, and its distribution depends primarily on the high energy photon density rather than gas density.

Using the 2.29 μm CO 2-0 bandhead we can resolve the nuclear star forming region, which has FWHM 0.22'' and 0.12'' at the 2 PAs, indicating a size scale of ~ 40 pc. The fraction of K-band light due to stars is determined from both the slope of the continuum and W_{CO} to be 20–30%. Based on the derived stellar luminosity, starburst models then indicate that the minimum mass of stars within a radius of 0.1'' is $1.5 \times 10^7 M_{\odot}$ (occurring if the age is only 10 Myr, when late type supergiants dominate the near infrared stellar continuum). The maximum mass is constrained by M_{dyn} to be $3.5 \times 10^7 M_{\odot}$, requiring an age no greater than 60 Myr. Thus, the stars in this cluster are very young, lie predominantly within the molecular gas ring at 0.2'', and account for most of the mass on this scale.

5. MASSIVE YOUNG STELLAR DISK IN MKN 231

The ultraluminous infrared galaxy Mkn 231, which at 170 Mpc distance has $L_{\text{bol}} \sim 3 \times 10^{12} L_{\odot}$, hosts an AGN that, with $M_{\text{B}} = -21.7$, is often classed as a QSO. However, it is now clear that a significant fraction of its luminosity in fact originates in star formation, making Mkn 231 a key object for investigations into whether or not ULIRGs evolve into QSOs. The structural and kinematic properties of this and other late stage ULIRG mergers have previously been studied to investigate whether they might evolve later into (intermediate mass, L_{*}) ellipticals⁹; and to test if, once rid of their gas and dust shells, they might be the progenitors of QSOs.¹⁸ As a sample, the ULIRGs appear to have elliptical-like properties: relaxed stellar populations with $r^{-1/4}$ radial

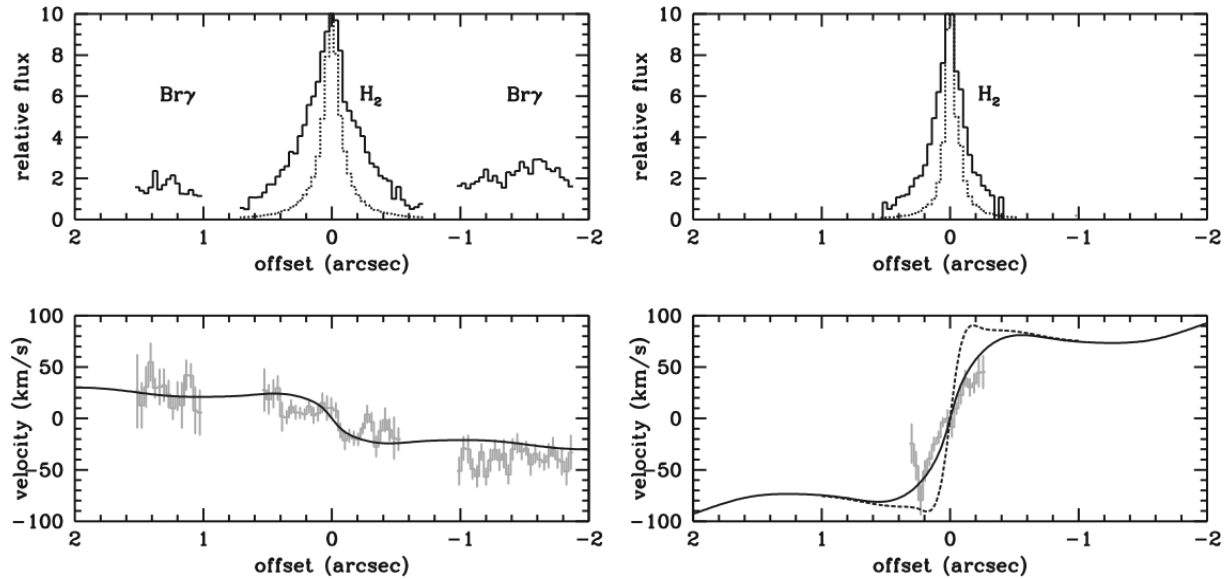


Figure 6. NGC 7469. Spatial (upper) and velocity (lower) profiles at PAs 33° (left) and 100° (right) for K-band emission lines. The continuum is shown in the upper panels (dotted line) for reference. Overplotted in the lower panels are the velocity curves from the mass model, which match the data well and show that on these scales the central mass is not compact (the dotted line in the lower right panel shows how the velocity curve would appear if it were).

luminosity profiles, and velocity dispersions of $\sim 180 \text{ km s}^{-1}$ with only moderate rotation. Based on numerical simulations of mergers between gas rich spirals, this is what one might expect since most ULIRGs, including Mkn 231, exhibit the huge tidal tails typical of such mergers. However, Mkn 231 presents a puzzle since its stellar velocity dispersion of 115 km s^{-1} is rather small, yielding both a low bulge mass and a low M_{BH} , which results in a highly super-Eddington AGN luminosity. Adaptive optics observations on the Keck II telescope, which are summarised here and described fully elsewhere,³ have resolved this problem.

If the mean stellar type dominating the nuclear stellar H-band continuum does not vary too much, the $1.63 \mu\text{m}$ CO 6-3 bandhead absorption ‘flux’ traces the spatial extent of the stars. Fig. 7 (left) shows that this profile is different to the continuum, which has a strong narrow core originating in dust heated by the AGN. Distinguishing between the de Vaucouleurs $r^{1/4}$ and exponential fits to the stellar profile is crucial for our understanding of the geometry of the star forming region. Hence in Fig 7 (right) we plot the logarithm of the profiles as functions of $r^{1/4}$, on which scaling the de Vaucouleurs profile appears as a straight line. It is then clear that an $r^{1/4}$ law does not match the data at larger radii, and that its effective radius r_e (defined as the boundary at within which half the total light is included) is inconsistent with the scales on which the star formation is seen. On the other hand, an exponential profile with scale length $r_d \sim 0.2''$ does match the data, indicating that the stars lie in a disk rather than a spheroid.

A nearly face-on ($i=10^\circ$) molecular disk is already known to exist in Mkn 231. We need to consider whether our result that the stars lie in the same disk is consistent with the seeing-limited stellar kinematics,¹⁸ for which $\sigma = 115 \text{ km s}^{-1}$ and $V_{\text{rot}}/\sigma = 0.2$. Using the properties of the molecular disk⁵ at $r = 0.6''$ ($V_{\text{rot}} \sin i = 60 \text{ km s}^{-1}$, $M_{\text{dyn}} = 12.7 \times 10^9 M_\odot$, scale height 23 pc) gives a mean velocity dispersion perpendicular to the disk plane of 80 km s^{-1} . Putting in also an exponential profile as above, accounting for seeing, and repeating the seeing-limited observations yields $\sigma = 107 \text{ km s}^{-1}$ and an apparent $V_{\text{rot}}/\sigma = 0.3$. This means that a nearly face-on stellar disk can – in the right circumstances – masquerade as a spheroid.

The fraction of H-band light due to stars is found from the equivalent width of the CO 6-3 bandhead, W_{CO} . The stellar luminosity one derives can then be used in starburst models, yielding a minimum mass (occurring when late type supergiants dominate the continuum, at an age of $\sim 10 \text{ Myr}$) of $1.3 \times 10^9 M_\odot$ out to $r = 0.6''$. The upper limit to the age and mass is set by M_{dyn} . At $0.6''$, we find $M_{\text{dyn}} = 6.7 \times 10^9 M_\odot$ (half of that derived for the cold gas,⁵ since we measure $V_{\text{rot}} \sin i = 40 \text{ km s}^{-1}$). Accounting for the gas mass leaves at most $4.3 \times 10^9 M_\odot$

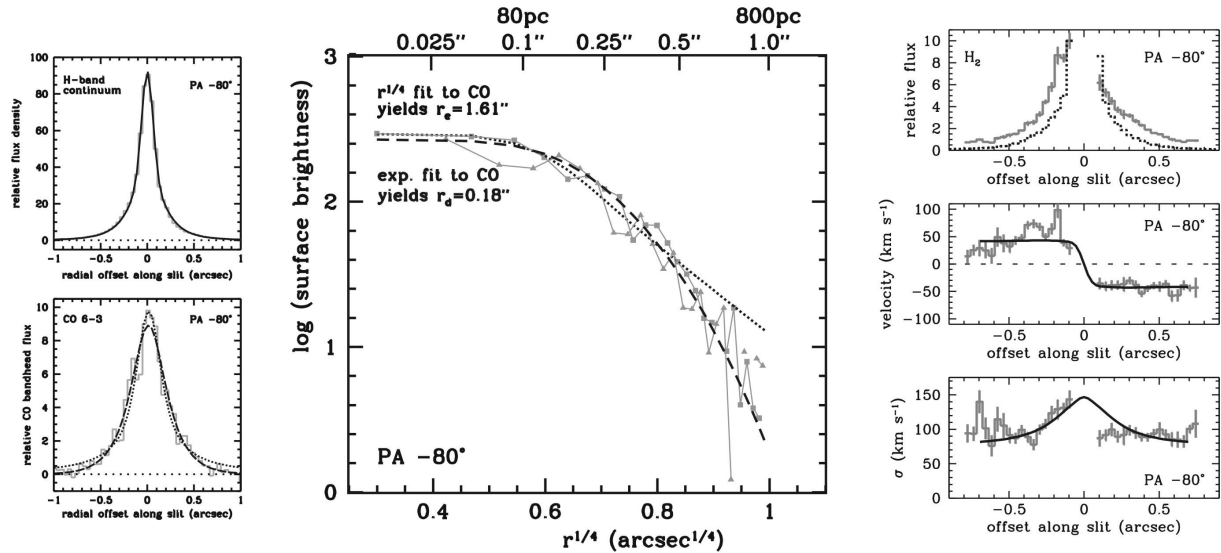


Figure 7. Mkn 231. Left: spatial profiles of the continuum (upper) and CO absorption ‘flux’ (lower) showing that the nuclear star forming region is resolved. Overplotted in the lower panel are $r^{1/4}$ (dotted) and exponential (dashed) profiles. Centre: logarithm of the CO profile as a function of $r^{1/4}$, showing that the exponential (dashed) profile is a better match than the $r^{1/4}$ (dotted), and hence that the stars reside in a disk rather than a spheroid. Right: flux profile (top), velocity (middle), and velocity dispersion (bottom) across the nucleus. The black curves show the observed rotation curve and velocity dispersion of the best fitting mass model.

of stars. Hence, from starburst models, the maximum age of the stars is 120 Myr. This remarkably young age is supported by other observations of PAH features,¹⁶ mid infrared emission lines,⁸ the infrared spectral energy distribution,²⁰ and the radio continuum.¹

Our results show that the stars we see lie in a disk rather than a spheroid, and so σ cannot be used to estimate M_{BH} . Being so young, it is likely that the stars formed *in situ* in the nearly face-on gas disk, which is itself a product of the merger that created Mkn 231.

CONCLUSIONS

The ‘standard’ way to measure the PSF (i.e. with a reference star) is unsatisfactory for AGN, particularly with spectroscopic data. Fortunately, there are a variety of other methods which can provide some indication of the important quantities: the spatial resolution and the amount of light still in the halo.

Deconvolving data is, for extragalactic work, often of limited use due to the low signal-to-noise of the data and diffuse nature of the object. However, as long as there is a physical model that one wishes to test, and which could describe the spatial morphology, a preferable alternative is to convolve the model with an estimate of the PSF. This has the advantages of providing a physical interpretation of the morphology, and giving a good indication of the range of models that could match the data.

Using these methods, we have analysed in detail H- and K-band data which clearly resolve the nuclear star forming regions in the centres of 2 type 1 AGN. Constraining starburst models using the fraction of stellar light determined from W_{CO} and the dynamics measured from the H₂ 1-0S(1) line (and, where possible, stellar features), indicates that the nuclear star forming regions are extremely young and constitute a significant fraction of the total mass on these scales. In Mkn 231 it is likely that the stars have formed in the molecular disk of scale length 150–200 pc which has resulted from the merger of gas rich spirals; in NGC 7469 the star cluster lies inside a molecular ring of radius 65 pc.

ACKNOWLEDGMENTS

The authors are grateful to the assistance and hospitality provided by the Observatories at Keck and Paranal.

REFERENCES

1. C. Carilli, J. Wrobel, J. Ulvestad, 1998, *AJ*, **115**, 928
2. R. Davies, L. Tacconi, R. Genzel, 2004, *ApJ*, **602**, 148
3. R. Davies, L. Tacconi, R. Genzel, 2004, *ApJ*, **613** (to appear in 1 Oct 2004 issue)
4. R. Davies, L. Tacconi, R. Genzel, N. Thatte, 2004, in preparation
5. D. Downes, P. Solomon, 1998, *ApJ*, **507**, 615
6. P. Erwin, A. Graham, N. Caon, 2003, in *Carnegie Observatories Astrophysics Series, Vol. 1: Coevolution of Black Holes and Galaxies*, ed. L.Ho
7. R. Genzel, L. Weitzel, L.E. Tacconi-Garman, M. Blietz, M. Cameron, A. Krabbe, D. Lutz, A. Sternberg, 1995, *ApJ*, **444**, 129
8. R. Genzel, D. Lutz, E. Sturm, E. Egami, D. Kunze, A. Moorwood, D. Rigopoulou, H. Spoon, A. Sternberg, L.E. Tacconi-Garman, L.J. Tacconi, N. Thatte, 1998, *ApJ*, **498**, 579
9. R. Genzel, L.J. Tacconi, D. Rigopoulou, D. Lutz, M. Tecza, 2001 *ApJ*, **563**, 527
10. D. Gratadour, Y. Clénet, D. Rouan, O. Lai, T. Forveille, 2003, *A&A*, **411**, 335
11. Jolissaint L., et al., 2004, this proceedings
12. Marino J., et al., 2004, this proceedings
13. J. Mazzearella, G. Voit, B. Soifer, K. Matthews, J. Graham, L. Armus, D. Shupe, 1994, *AJ*, **107**, 1274
14. A. Prieto, et al., 2004, *ApJ*, submitted
15. Rigal F., et al., 2004 this proceedings
16. D. Rigopoulou, H. Spoon, R. Genzel, D. Lutz, A. Moorwood, Q. Tran, 1999, *AJ*, **118**, 2625
17. D. Rouan, et al., 2004, *A&A*, **417**, L1
18. L.J. Tacconi, R. Genzel, D. Lutz, D. Rigopoulou, A.J. Baker, C. Iserlohe, M. Tecza, 2002, *ApJ*, **580**, 73
19. N. Thatte, A. Quirrenbach, R. Genzel, R. Maiolino, M. Tecza, 1997 *ApJ*, **490**, 238
20. A. Verma, 1999, *PhD Thesis*, Imperial College, London
21. L. Wallace, K. Hinkle, 1997, *ApJS*, **111**, 445
22. R. Weiss, S. Hippler, M. Feldt, 2003, in *Science with Adaptive Optics*, ed. W. Brandner, M. Kasper
23. M. Wittkowski, Y. Balega, T. Beckert, W. Duschl, K.-H. Hofmann, G. Weigelt, 1998, *A&A*, **329**, L45